ISSN 2347 - 3983
Volume 8. No. 8, August 2020
International Journal of Emerging Trends in Engineering Research
Available Online at http://www.warse.org/IJETER/static/pdf/file/ijeter75882020.pdf
https://doi.org/10.30534/ijeter/2020/75882020

Design of Decoupled Current Controller for Grid Connected Modular Multilevel Converter

K. Shivashanker[1], M. Janaki[2]
[1] Research Scholar, School of Electrical Engineering, Vellore Institute of Technology, Vellore, Tamil Nadu, India, kondoorushiva@gmail.com
[2] Associate Professor, School of Electrical Engineering, Vellore Institute of Technology, Vellore, Tamil Nadu, India, janaki.m@vit.ac.in

ABSTRACT

Modular multilevel converter (MMC) becomes furthermost promising topologies especially for medium or high voltage (HV) applications. A typical application of MMC is to control the active power as well as reactive power. This paper presents the design of decoupled current controller for a grid connected MMC. The proposed controller gives an efficient and decoupled control of active power and reactive power then substantially improves MMC dynamic response. However, the performance of MMC depends on the controller's parameters. The tuning of controller's parameters depends on the desired output for disturbance applied to the input. The effectiveness of MMC is evaluated by transient simulation with decoupled current controller parameters. The transient simulation is done by MATLAB/Simulink using three-phase detailed model.

Key words: Decoupled current controller, half-bridge sub-module (HBSM), high voltage direct current (HVDC) transmission system, modular multilevel converter (MMC).

1. INTRODUCTION

The conventional HVDC transmission system uses thyristors for the satisfactory operation, which depends upon ac network voltage. The typical limitation of classical HVDC transmission is a failure of commutation and weak ac systems are difficult to run. The two-level voltage source converter (VSC)-HVDC systems have many advantages compared to traditional HVDCs, such as converter bus dynamic voltage support, active power and reactive power can regulate independently, power reversal can possible without altering the polarity of a dc voltage, the possibility to supply a frail ac system, and no need for rapid communication between required two station converters [1]. However, in VSC topology, losses are unequally shared by both inner and outer loops. The demerits of two-level VSC is conquered by multilevel converter topologies.

Multilevel converters (MLCs) comprise power- semiconductor devices array and dc source voltages, the output where stepped waveform voltages produce. The multilevel voltage source converter allows incorporating output voltages of minimal harmonic distortion, unlike a two-level VSC. In multilevel converters by increasing the levels number, the voltage output waveform has been produced in the form of a staircase having more steps with minimized harmonic distortion. Nonetheless, the number of devices are increasing with a large number of levels which need to controlled and the complexity of control [2]. So that, modular multilevel converter was proposed in [3] to overwhelm the demerits of multilevel converters.

An MMC is a finest power electronic converter extended to be most suitable for medium voltage (MV) and HV (or power) applications such as HVDC transmission system, flexible ac transmission systems (FACTS), medium voltage variable motor drives [4], and energy storage systems [4], [5]. MMC has distinctive features compared with multilevel voltage source converter topologies such as modularity construction, high reliability, less switching losses, and better output waveforms.

In [6], A traditional two-level VSC control the positive-sequence and negative sequence current components only. In 3-level neutral point clamped (3L-NPC) converter partially control the zero-sequence current components with suitable selection of redundant switching state vectors. However, in the VSC-based HVDC system, a zero-sequence current components typically ignored from a converter with the suitable transformer connection, Y-Δ and Δ on the converter side but under an unbalanced faults on a converter transformer are unavoidable. In [7], modular multilevel converters controlled by pulse-width modulation (PWM) method and space-vector modulation (SVM) method resulting in high-frequency switching losses. Therefore both methods are not suitable to the HV (or power) applications. To minimize switching losses, an active-harmonic-elimination (AHE) scheme is used, which is the most remarkable advancement to selective-harmonic-elimination (SHE) scheme. Nonetheless, in HVDC system applications, for a large number of sub-modules numerical algorithm complexity increases. The aforementioned demerits overwhelm by nearest level control (NLC) scheme, which is most suitable for high-level converters. In [8], model predictive control (MPC) method is proposed for the back-to-back HVDC transmission system. This enables regulation of the active power and reactive power, voltages of capacitor balancing achievement and minimize the circulating currents.

In this paper, four half-bridge sub-modules in each (upper & lower) arm per phase leg of MMC is considered and presents the designing of a decoupled current controller, which gives an effective control structure for the active power and reactive

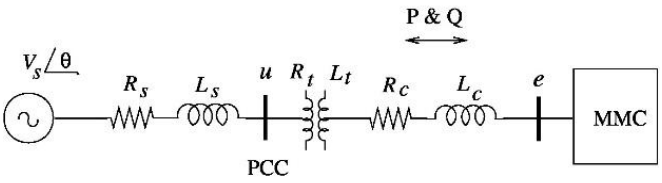

Figure 1: Single line diagram of MMC connected to grid.

power/current and improves the MMC dynamic performance. The performance of MMC based on the controller parameters, which depend on the desired output for the disturbance applied to an input. The effectiveness of an MMC is assessed by the transient time-domain simulation, and the result shows a better transient response.

The paper organized as: the section II explores modeling of grid connected MMC. Section III describes the design of decoupled current controller for MMC. Section IV explores Modeling of system in MATLAB/Simulink and result analysis. Section V conclude the paper.

2. MODELING OF GRID CONNECTED MMC

Single line diagram of MMC connected to grid is illustrated in Figure 1. R_C and L_C are connecting resistance and inductance respectively. R_t and L_t are leakage resistance and leakage inductive reactance of interfacing transformer of the modular multilevel converter. R_S and L_S are source resistance and source inductance.

Figure 2 depicts the schematic representation of 3-Φ detailed model of MMC, which comprises three legs and each leg consisting of upper arm & lower arm. Each arm consisting n identical cascaded half bridge SMs and an arm inductor. The SM comprises two power electronic devices (i.e., IGBTs) and one shunt capacitor is shown in Figure 3. The two IGBTs are operated in complementary with corresponding gate signals. The output voltage of HBSM, $V_{SMout} = V_{cap}$ for the upper device is ON and $V_{SMout} = 0$ for the lower device is ON.

From Figure 2, MMC arm currents and output voltages are given by

$$i_{xl} = -\frac{i_x}{2} + i_{diffx}$$

$$i_{xu} = \frac{i_x}{2} + i_{diffx} \qquad (x= a, b, c) \qquad (1)$$

$$e_x = u_x - R_{eq} i_x - L_{eq} \frac{di_x}{dt} \qquad (2)$$

Where $R_{eq} = R_c + \frac{R}{2}$ and

$$L_{eq} = L_c + \frac{L}{2}$$

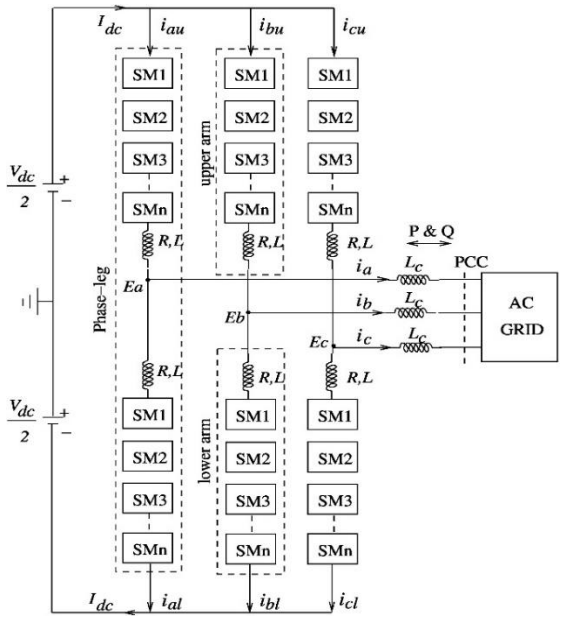

Figure 2: Schematic diagram of MMC [9]

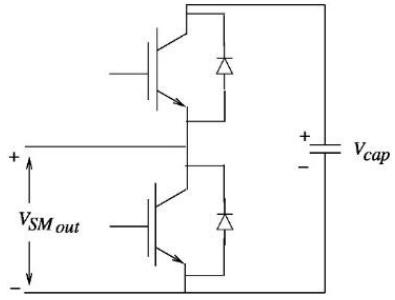

Figure 3: Half-bridge SM structure [9]

R & L are arm resistor and arm inductor. i_{xl} and i_{xu} are the lower arm and upper arm currents of phase x (x=a, b, c). i_x is ac side current of phase x. e_x is the MMC output voltage. u_x is the voltage of ac-side. i_{diffx} is the phase x unbalanced current, which can expressed as

$$i_{diffx} = \frac{(i_{xl} + i_{xu})}{2} = \frac{I_{dc}}{3} + i_{cirx} \qquad (3)$$

where I_{dc} is a dc-line current and i_{cirx} is a circulating current of phase x.

From Figure 2, relationship between arm voltages and dc voltages can be given as

$$\frac{V_{dc}}{2} = \frac{(u_{xl} + u_{xu})}{2} + Ri_{diffx} + L\frac{di_{diffx}}{dt} \qquad (4)$$

where V_{dc} is voltage of the dc-line. u_{xl} and u_{xu} are the lower arm voltage and upper arm voltage respectively of phase x.

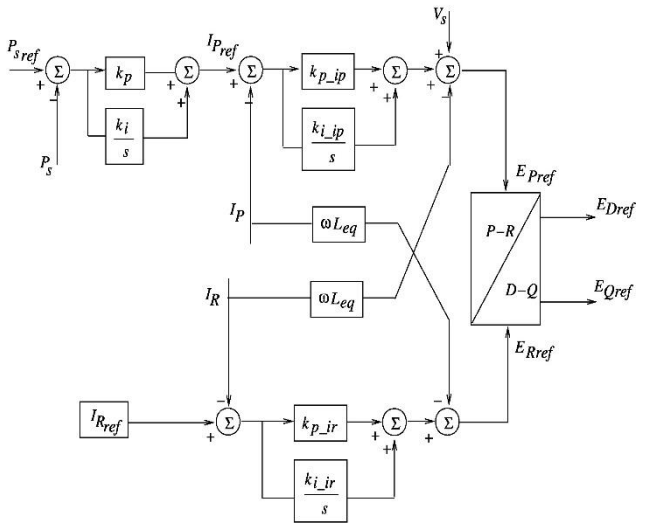

Figure 4: The structure of decoupled current controller for grid connected MMC [10]

3. DESIGN OF DECOUPLED CURRENT CONTROLLER

The pictorial representation of decoupled current controller for MMC is shown in Figure 4. The main objective of controller such that, independent regulation of active and reactive power. From Figure 4, it is noticed that, the real (or active) current reference value (I_{Pref}) of MMC is obtained from power controller and the MMC reactive reference current (I_{Rref}) is kept to be constant or set by the ac voltage controller to maintain specific magnitude of ac bus voltage value [11]. The actual active and reactive currents of MMC obtained from D-Q component currents of MMC. The proposed controller gives an efficient and decoupled regulation of active power and reactive power then significantly improves the MMC dynamic response. However, the MMC response depends on the controller's parameters, which are tuned based on desired output for disturbance applied to the input.

The MMC output voltage presented in the D-Q frame of reference [12] as follows:

$$E = \sqrt{(E_D^2 + E_Q^2)} \quad (5)$$

$$E_D = E_R cos\theta + E_P sin\theta \quad (6)$$

$$E_Q = -E_R sin\theta + E_P cos\theta \quad (7)$$

where E_D, E_Q are D-Q output voltage components of MMC. E_P and E_R are real and reactive voltages of MMC respectively.

From Figure 4, the real and reactive currents [13] are given by

$$I_P = I_D sin\theta + I_Q cos\theta \quad (8)$$

$$I_R = -I_D cos\theta + I_Q sin\theta \quad (9)$$

where θ is phase angle of reference bus voltage. I_D, I_Q are D-Q output current components of MMC.

4. MODELLING OF SYSTEM IN MATLAB/SIMULINK AND RESULT ANALYSIS

The simulation of MMC model is developed in MATLAB/Simulink to validate the performance of the decoupled current controller. In simulation model, a phase-shifted carrier modulation based PWM method (PSC-PWM) employed to generate gate signals. Figure 5 illustrates the simulation model and the decoupled current control method for grid connected MMC. In real-time applications, the MMC voltage of ac-side (usually referred to as the PCC voltage) is to be stipulated (or constant). So that, the transferred active power and reactive power from ac grid to MMC and vice versa can be influenced by ac-side current. Therefore the ac-side MMC current control is equal to control of transferred power [9]. A control scheme of active current and reactive current is presented in Figure 4. In Figure 5, θ and ωt are phase angle and ramp of the reference bus voltage. In this paper, it is assumed to 1+j0. The 3-Φ voltage and currents are transforming to D-Q frame by using Park transformation to further.

The fundamental frequency Park transformation is given by

$$P_1 = \sqrt{\frac{2}{3}} \begin{bmatrix} cos(\omega t) & cos(\omega t - \frac{2\pi}{3}) & cos(\omega t + \frac{2\pi}{3}) \\ sin(\omega t) & sin(\omega t - \frac{2\pi}{3}) & sin(\omega t + \frac{2\pi}{3}) \end{bmatrix} \quad (10)$$

A Phase-locked loop (PLL) is a technique and used to obtain the information about voltage. So far, many PLLs has been proposed. Among that, the synchronous rotating frame PLL (SRF-PLL) is mostly used, which is quite simple and is suitable for use in single and three-phase systems. Under ideal conditions of grid (excluding harmonics) and unbalance of system, SRF-PLL attain a quick and accurate grid voltage frequency and phase angle [14].

The grid D-Q component voltages (V_{sD} & V_{sQ}) and converter D-Q component currents (I_D & I_Q) are obtained with help of eq. (10). From Figure 5, the actual active power (P_S) and reactive power (Q_S) calculated from grid D-Q component voltages and converter currents are noticed. The proposed decoupled current control method tune the controller parameters based on desired output for a disturbance applied to an input.

The simulations of a 3-Φ detailed model of MMC is carried out by time-domain transient analysis under two different step disturbances. The transient analysis is carried out for the step disturbance in the reference value employed at 0.50 sec and restored at 1.0 sec. The following subsections present the transient simulation for step disturbance in the active power reference and reactive current reference.

4.1 Step disturbance in active power reference (P_{Sref})

Step response of the active current (I_P) for a three-phase detailed model of MMC after applying the proposed scheme with reversal of active power reference (P_{Sref}) is depicted in Figure 6. From Figure 6, it is noticed that the step disturbance in P_{Sref} value is employed at 0.50 sec and restored at 1.0 sec, and result shows the active current (I_P) has followed the disturbance applied to the input. Figure 7 shows the step response of active power (P) for a three-phase detailed MMC model after applying the decoupled

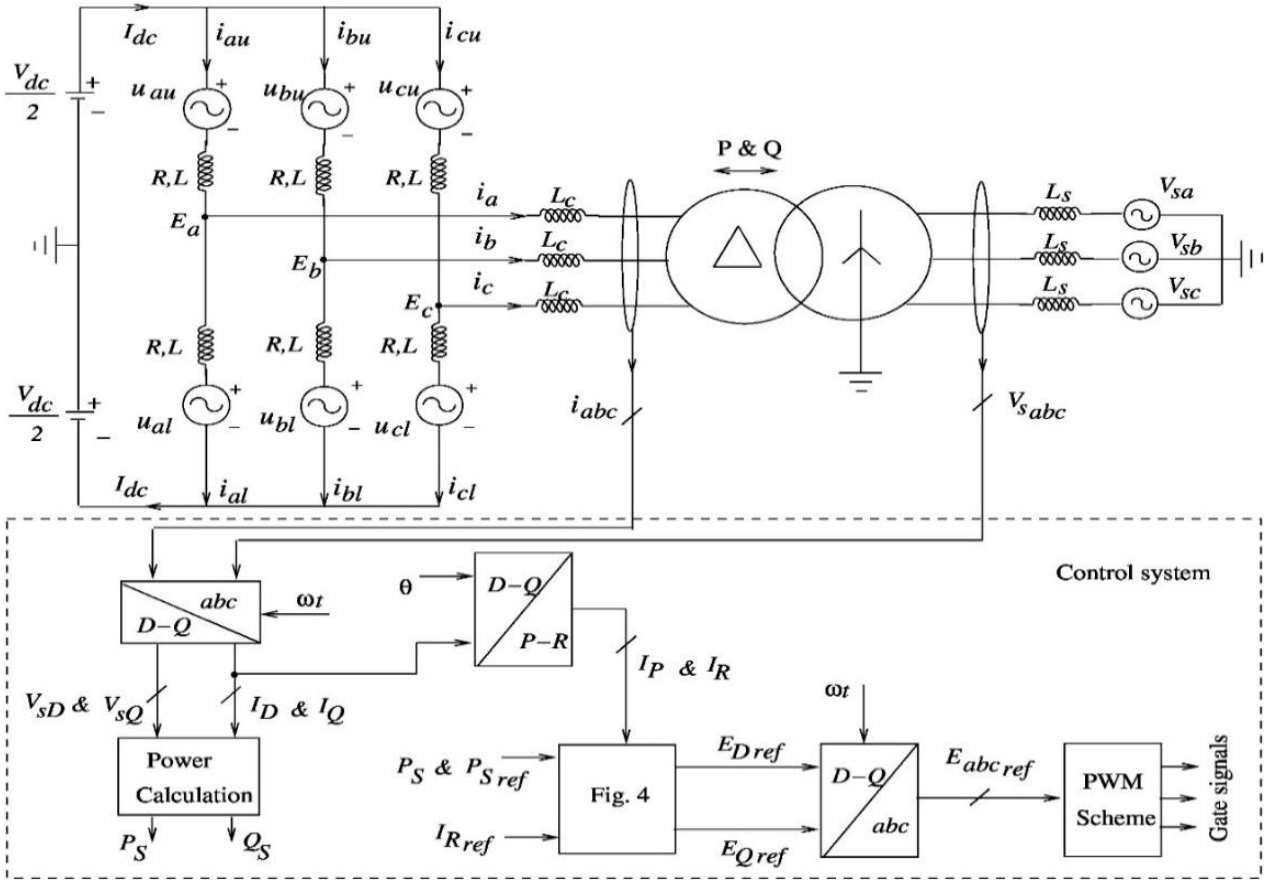

Figure 5: Simulation model of grid connected MMC with decoupled current control method [9]

current control scheme with reversal of P_{Sref}. From Figure 7, it is clear that the step disturbance in P_{Sref} value is employed at 0.50 sec and restored at 1.0 sec, and result shows the active power (P) has followed the disturbance applied to the input.

Figure 8 depicts the step response of reactive current (I_R) for a three-phase detailed model of MMC after applying the current decoupled controller with a reversal of active power reference (P_{Sref}). From Figure 8, it is clear that reactive current (I_R) hasn't affected the disturbance applied to the input (or remain unchanged). Figure 9 illustrates the step response of reactive power (Q) for a three-phase detailed model of MMC after applying the proposed scheme with reversal of P_{Sref}. From Figure 9, it is clear that reactive power (Q) hasn't affected the disturbance applied to the input (or remain unchanged).

4.2 Step disturbance in reactive current reference (I_{Rref})

Step response of the active current (I_P) of a 3-Φ detailed MMC model with the current decoupling controller for a step disturbance in reactive current reference (I_{Rref}) is illustrated in Figure 10. From Figure10, it is noticed that the result hasn't affected from step disturbance in I_{Rref} value.

Figure 11 shows the step response of active power (P) for a three-phase detailed model of MMC after applying the current decoupling Controller for a step disturbance in I_{Rref}. From Figure 11, it is noticed that the result hasn't affected from step disturbance in I_{Rref} value.

The step response of the reactive current (I_R) of a 3-Φ detailed MMC model with the current decoupling controller for a step disturbance in I_{Rref} is illustrated in Figure12. From Figure 12, it is noticed that the step disturbance in I_{Rref} value is employed from 0.50 sec to 1.0 sec. The result shows the reactive current (I_R) has followed the disturbance applied to the input.

Figure 13 explores the step response of reactive power (Q) for a three-phase detailed model of MMC after applying the

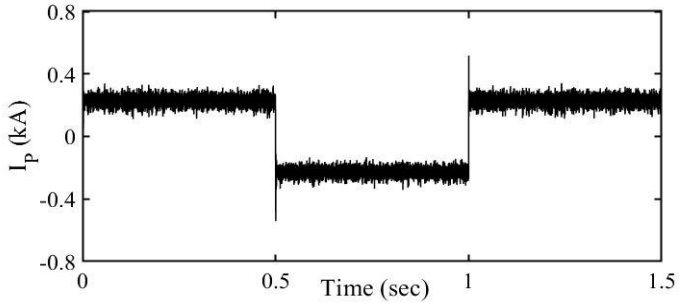

Figure 6: Response of active current (I_P) for step disturbance in P_{Sref}.

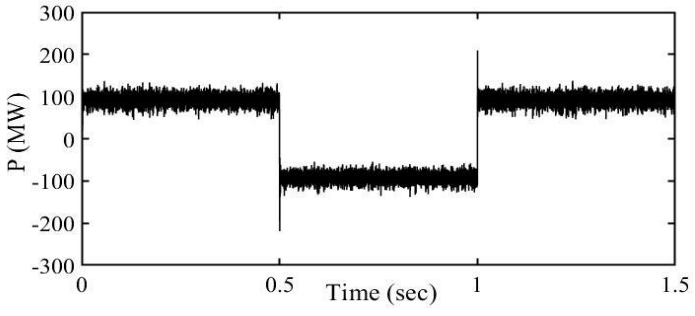

Figure 7: Response of active power (P) for step disturbance in P_{Sref}.

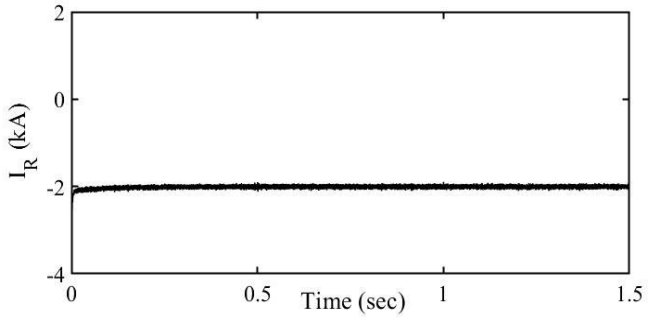

Figure 8: Response of reactive current (I_R) for step disturbance in P_{Sref}.

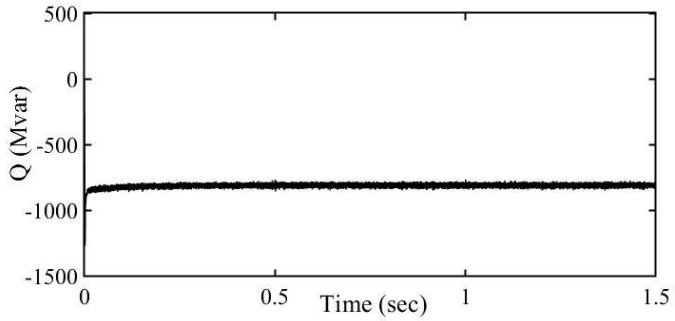

Figure 9: Response of reactive power (Q) for step disturbance in P_{Sref}.

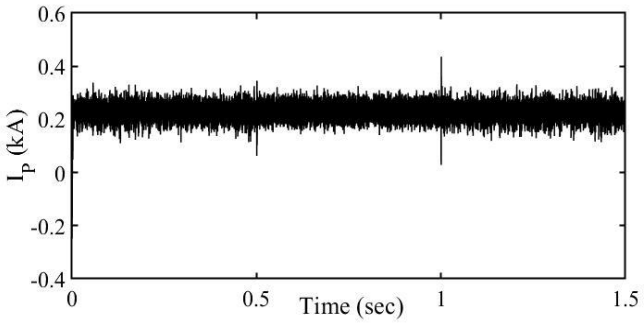

Figure 10: Response of active current (I_P) for step disturbance in I_{Rref}.

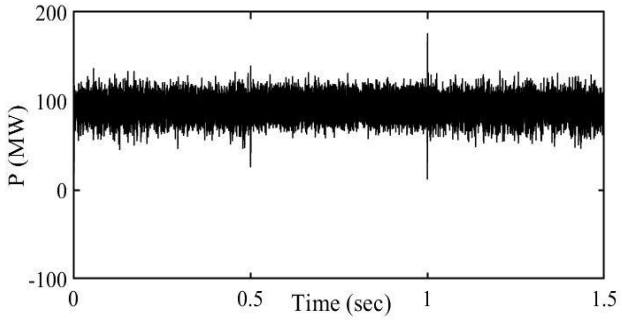

Figure 11: Response of active power (P) for step disturbance in I_{Rref}.

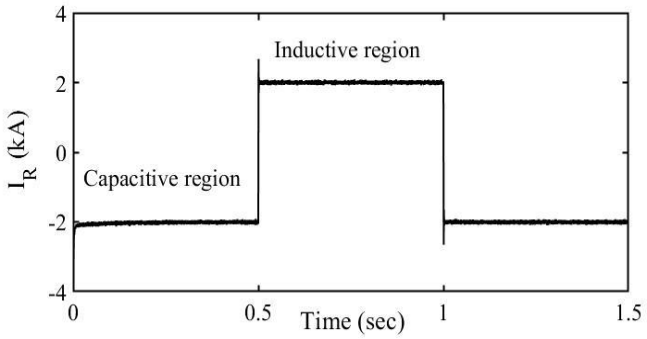

Figure 12: Response of reactive current (I_R) for step disturbance in I_{Rref}.

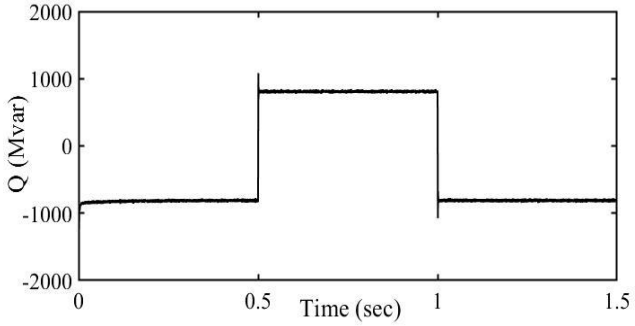

Figure 13: Response of reactive power (Q) for step disturbance in $I_{Rref.}$

current decoupled control scheme for a step disturbance in I_{Rref}. From Figure 13, it is clear that the step disturbance in I_{Rref} value is employed at 0.50 sec and restored at 1.0 sec. The result shows the reactive power (Q) has followed the disturbance applied to the input.

Figure 14 presents a phase relation between phase-a voltage of grid and phase-a current of converter for step disturbance in I_{Rref}. From Figure 14(b), it is noticed that the phase current

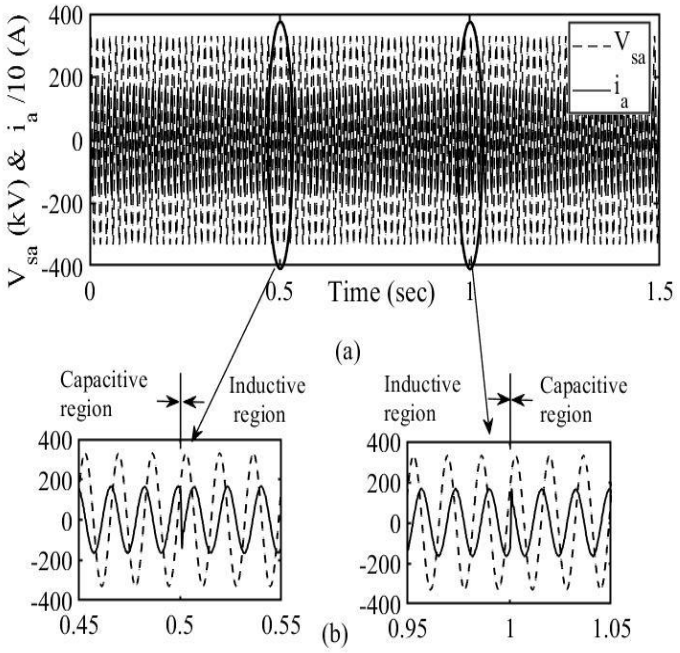

Figure 14: Phase voltage of grid & converter current for step disturbance in I_{Rref}. (a) Overall view, (b) Zoom view.

of converter changing from leading to lagging for the reactive current reference switching from capacitive to inductive mode at 0.50 sec. Following this, the converter current changes from lagging to leading for the reactive current reference switching from inductive to capacitive mode at 1.0 sec. Referring to Figures 12 & 14, it is noticed that, step response of the MMC reactive current with the proposed controller's parameters, undergo smooth and fast transition from between capacitive mode and inductive mode of the MMC operation, and finally reaches the steady-state less than 0.003 sec.

5. CONCLUSION

This paper proposes design of a decoupled current controller for the modular multilevel converter. The proposed control scheme can achieve an independent regulation of active power and reactive power, also significantly improve the MMC performance. The proposed decoupled current control scheme parameter's selection is based on the desired output for a disturbance applied to the input. The performance of an MMC with the proposed controller's scheme is evaluated by transient time-domain simulation, which is noticed that the MMC with controller's parameters shows a good transient results.

REFERENCES

1. N. Prabhu and K. R. Padiyar. **Investigation of Subsynchronous Resonance With VSC-Based HVDC Transmission Systems,** *IEEE Transactions on Power Delivery*, Vol. 24, no. 1, pp. 433-440, Jan. 2009.
2. M. F. Kangarlu, and E. Babaei. **A Generalized Cascaded Multilevel Inverter Using Series Connection of Submultilevel Inverters,** *IEEE Transactions on Power Electronics*, vol. 28, no. 2, pp. 625-636, Feb. 2013.
3. Lesnicar, and R. Marquardt. **An innovative modular multilevel converter topology suitable for a wide power range,** *IEEE Bologna Power Tech Conference Proceedings*, vol. 3, June 2003.
4. J. Wang, Y. Tang, and X. Liu. **Arm Current Balancing Control for Modular Multilevel Converters Under Unbalanced Grid Conditions,** *IEEE Transactions on Power Electronics*, vol. 35, no. 3, pp. 2467-2479, March 2020.
5. Ahmad Abid Mazlan, Norzanah Rosmin, Anita Ahmad, and Aede Hatib. **Compressed Air Energy Storage System for Wind Energy: A Review,** *International Journal of Emerging Trends in Engineering Research*, vol. 8, no. 7, pp. 3080-3087, July 2020. https://doi.org/10.30534/ijeter/2020/34872020
6. M. Guan, and Z. Xu. **Modeling and Control of a Modular Multilevel Converter-Based HVDC System Under Unbalanced Grid Conditions,** *IEEE Transactions on Power Electronics*, vol. 27, no. 12, pp. 4858-4867, Dec. 2012.
7. Q. Tu, and Z. Xu. **Impact of Sampling Frequency on Harmonic Distortion for Modular Multilevel Converter,** *IEEE Transactions on Power Delivery*, vol. 26, no. 1, pp. 298-306, Jan. 2011.
8. J. Qin, and M. Saeedifard. **Predictive Control of a Modular Multilevel Converter for a Back-to-Back HVDC System,** *IEEE Transactions on Power Delivery*, vol. 27, no. 3, pp. 1538-1547, July 2012.
9. J. Wang, and P. Wang. **Power Decoupling Control for Modular Multilevel Converter,** *IEEE Transactions on Power Electronics*, vol. 33, no. 11, pp. 9296-9309, Nov. 2018.
10. M. Janaki, Nagesh Prabhu, R. Thirumalaivasan, and D.P. Kothari. **Mitigation of SSR by Subsynchronous Current Injection with VSC HVDC,** *International Journal of Electrical Power & Energy Systems*, vol. 57, pp. 287 - 297, May 2014.
11. H. Saad et al. **Dynamic Averaged and Simplified Models for MMC Based HVDC Transmission Systems,** *IEEE Transactions on Power Delivery*, vol. 28, no. 3, pp. 1723-1730, July 2013.
12. S. Venkateswarlu, and M. Janaki. **Analysis and Mitigation of Multimodal SSR using Kalman Filter based SSDC in Non-identical Generators,** *International Journal of Emerging Trends in Engineering Research*, vol. 8, no. 7, pp. 3834-3839, July 2020.
13. Srikanth Velpula, R. Thirumalaivasan, and M. Janaki. **Stability Enhancement of STATCOM using Flower Pollination Algorithm,** *International Journal of Engineering & Technology, (IJET)*, vol. 7, no. 4.10, pp. 206-211, 2018.

https://doi.org/10.14419/ijet.v7i4.10.20897

14. J. Wang, J. Liang, F. Gao, L. Zhang, and Z. Wang. **A Method to Improve the Dynamic Performance of Moving Average Filter-Based PLL,** *IEEE Transactions on Power Electronics*, vol. 30, no. 10, pp. 5978-5990, Oct. 2015.